KSME Journal, Vol. 7, No. 4, pp. 372~388, 1993

# Trunk and Lower Extremity Muscle Activity in Seated Weight-Moving Tasks : Three-Dimensional Analyses of Intersubject and Intertask Differences

**Kwon Son* and James A. A. Miller****

*(Received April 6, 1993)*

A three-dimensional musculoskeletal model was used to predict the trunk and lower extremity muscle activity required to stabilize the body while performing dynamic tasks in the seated posture. We studied seven subjects performing four tasks consisting of cyclic or single-directional movements of a hand-held weight in the sagittal plane. Five different optimization schemes involving the minimization of muscle forces, muscle stresses, or joint force components were used to predict the 64 muscle force-time histories. A quantitative method was used to compare prediction schemes by correlating predicted muscle forces with measured myoelectric data and ranking the efficacy of each scheme for different tasks and subjects. The results showed that (1) the trunk and lower extremity muscles play an important role in stabilizing the seated posture in these tasks, (2) the most successful muscle force prediction scheme was not the same for all seven subjects performing a given task, or for a given subject performing all four tasks, and (3) these linear optimization techniques successfully predicted activity in up to 10 of the 15 muscles whose myoelectric signals were actually monitored.

**Key Words :** Trunk, Lower Extremity, Musculoskeletal Model, Muscle Activity, Seated Dynamic Tasks, Optimization Schemes, Myoelectric Signals

## 1. Introduction

The seated posture is fundamental to many work, school, transportation, and recreational activities. However, surprisingly little is known about how stable sitting is established and maintained by the neuromuscular control system. Such knowledge can lead to improved workplace design for healthy individuals as well as better clinical management of non-ambulatory patients.

Previous studies of sitting have included postural (Schobert, 1962 ; Bendix, 1984), myoelectric (Knutsson et al., 1966 ; Andersson, 1974), seat pressure (Bader and Hawken, 1986), and quasi-static biomechanical analyses (Andersson et al., 1980 ; Occhipinti et al., 1985). In previous work we have used planar biomechanical models to verify the importance of the lower extremities in stabilizing the seated posture (Son et al., 1988) and to explore the mechanical demands placed upon the trunk and lower extremity muscles in dynamic tasks performed in the seated position (Son and Miller, 1988). Such models have several limitations, including the two-dimensional representations of muscles and their lines of actions, and the restriction of tasks and motions to a single plane.

Due to the redundancy problem, muscle force predictions in biomechanical models are traditionally made using several optimization schemes (Seireg and Arvikar, 1973 ; Penrod et al., 1974 ; Crowninshield, 1978 ; Hardt, 1978 ; Pedotti et al., 1978 ; Crowninshield and Brand, 1981 ; Patriarco et al., 1981 ; Schultz et al., 1982 ; An et al., 1984 ; Röhrle et al., 1984 ; Davy and Audu, 1987).

* Department of Mechanical Engineering/Research Institute of Mechanical Technology, Pusan National University, Pusan 609-735, Korea

** Department of Mechanical Engineering and Applied Mechanics, University of Michigan, Ann Arbor, MI 48109-2125, U.S.A.

However, their efficacy has only recently been quantitatively evaluated for different subjects performing the same task (Son and Miller, 1988 ; Son, 1990).

The objective of this study, therefore, was to use a three-dimensional biomechanical model of the seated human to analyze bilateral joint loading and muscle activities in four similar, yet different weight-moving tasks. Five different linear optimization schemes were used to predict trunk and lower extremity muscle forces in each of seven subjects ; the efficacy of each scheme was evaluated quantitatively by comparing predicted forces with measured myoelectric (EMG) signals using a time correlation method (Son, 1990). Particular attention was paid to bilateral and intertask differences.

## 2. Materials and Methods

### 2.1 Test protocol

Experiments were performed on seven healthy young male subjects at the Biomechanical Laboratory of the University of Michigan. They were selected to match those studied by McConville et al.(1980), for whom anthropometric properties are available. Mean (SD) subject ages, statures, and weights were 27.9 (3.5) years, 178.8 (5.8) cm, and 726.9 (49.1) N, respectively.

Four weight-moving tasks were performed by each subject : a cyclic, sagittally-symmetric task with both hands (Task 1) ; a cyclic, right-handed task (Task 2) ; a right-handed, arm-stretching task (Task 3) ; and a right-handed, arm-folding task (Task 4). A weight of 2 kg mass was used in the two-handed task, while a weight of 1kg mass was used in all three right-handed tasks. Each seated task consisted of moving a weight with either one or both hands at shoulder height between the full flexion position (FFP) and the full extension position (FEP) of the arm elements in the sagittal plane (Fig. 1). Tasks 1 and 2, cyclic tasks, consisted of moving a hand-held weight from FFP via FEP and back to FFP in a repetitive, cyclic fashion at a frequency of 1 Hz. Task 3 consisted of moving the weight in a single direction from FFP to FEP, while in Task 4 the weight was moved in the opposite direction from FEP to FFP. Both Tasks 3 and 4 consisted of three parts : 0.25 second of static weight-holding, 0.5 second of weight-moving in a single direction, and 0.25 second of static weight-holding. Each task was performed in the sagittal plane and movements were cued by the beat of a metronome. At least five trials were performed for each task from which a single movement cycle that best satisfied the above task constraints was analyzed.

Detailed descriptions of the motion measurement (locations of upper body and extremity markers collected at 300 Hz using a CODA-3 system), foot-floor reaction measurement (reaction components collected at 30 Hz using an AMTI force plate beneath each foot), myoelectric (EMG) signal measurement (more than three seconds data collected at 900 Hz from each surface electrode) were given in our previous studies (Son, 1988 ; Son et al., 1988 ; Son and Miller, 1988), where data selection and analysis were also described in detail.

Fifteen large and superficial muscles on the right side of the trunk and right lower extremity were selected for the simultaneous recording of surface EMG activity during each seated task. These muscles included multifidus (MUL), rectus abdominis (RAB), medial external oblique (M EO), tensor fasciae latae (TFL), gluteus maximus

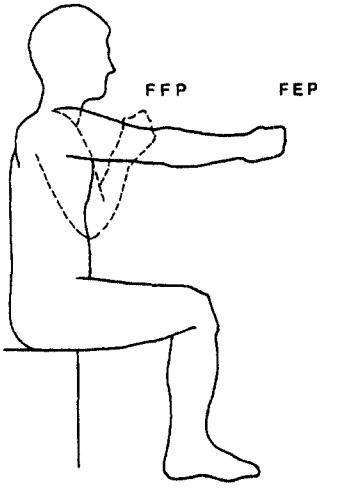


**Fig. 1** Extreme arm positions of a seated task

(GMA), adductor longus (ADD), rectus femoris (RFM), biceps femoris longus (BFL), semitendinosus (STN), sartorius (SAR), biceps femoris short head (BFS), gastrocnemius lateralis (GAL), soleus (SOL), peroneus longus (PER), and tibialis anterior (TAN).

### 2.2 Dynamic model

The seated human body was modelled as a three-dimensional system of fifteen rigid links connected by frictionless articulations (Fig. 2). The basic assumptions used were that (1) main body segments, such as head and neck, trunk, and pelvis, moved only in the sagittal plane, (2) upper extremity segments carrying a weight moved in a single vertical plane, (3) in a right-handed weight-moving task, every point of the left upper extremity segment moved with the same velocity and acceleration as the center of the left shoulder joint, (4) lower extremity segments remained fixed with constant flexion angles between the segments during all phases of a task, and (5) distributed reaction forces and moments acting through the floor and the seat could be replaced by equivalent point quantities. The body motion, which described each task, was analyzed using an inverse dynamics formulation for joint loadings of the trunk and lower extremities (Son et al., 1988; Son, 1990).

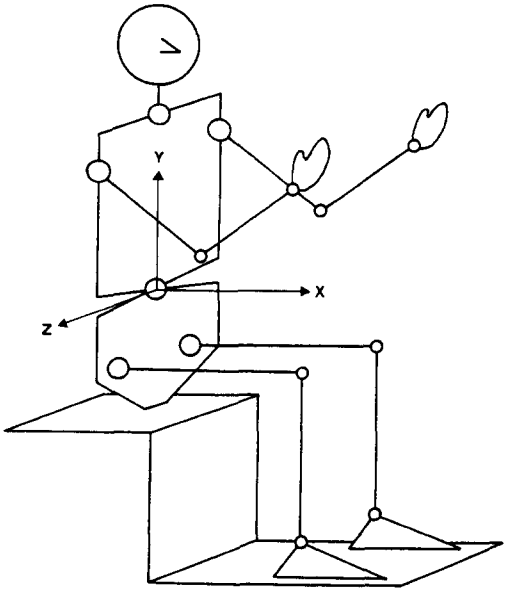


**Fig. 2** Schematic representation of links of the seated human body with x, y, and z-axes in a global coordinate system

### 2.3 Muscle model

A three-dimensional trunk and lower extremity muscular system was modelled using 64 single equivalent muscles: 22 trunk and 42 lower extremity muscles on both sides of the trunk and lower extremities. The basic assumptions used were (1) change in length of a trunk or lower extremity muscle was negligible in a seated task, (2) most muscles could be adequately described by a muscle model with a straight line-of-action, but a two-segment straight-line model was used for the tensor fasciae latae due to the hip flexion in the seated position, (3) the gluteal groups could be described by a curved-line model with a moment arm length reported by Németh and Ohlsén(1985), (4) the effect of passive elements, such as ligaments and articulated surfaces, was negligible at the trunk and hip joints so that internal moments are produced only by muscle contractions at these joints, and (5) the passive elements could develop resistance about the knee in varus-valgus and internal-external rotation, and about the ankle in internal-external rotation.

Trunk muscles were represented by 11 pairs of single equivalent muscles at the L3 level (Fig. 3) as in the validated model by Schultz et al.(1983). For consistency, their anatomical cross-sectional areas, lines of action, and locations of centroid for each trunk muscle were taken from their study.

The lower extremity muscles were idealized by 21 pairs of single equivalent muscles on each side (Fig. 3). They represented the muscles which have functional importance in three-dimensional joint stability or have substantial cross-sectional areas. The physiologic cross-sectional area (PCSA) of each muscle was calculated by scaling data reported by Brand et al.(1986). The rectus femoris and the vasti (interalis, medialis, and lateralis) were modelled as a single quadriceps equivalent, QUA, proximal to the patella and as a single patellar tendon equivalent, PAT, distal to the patella as in our previous study (Son and Miller, 1988).

The single equivalent muscles at hip joint were iliopsoas (PSO), iliacus (CUS), tensor fasciae

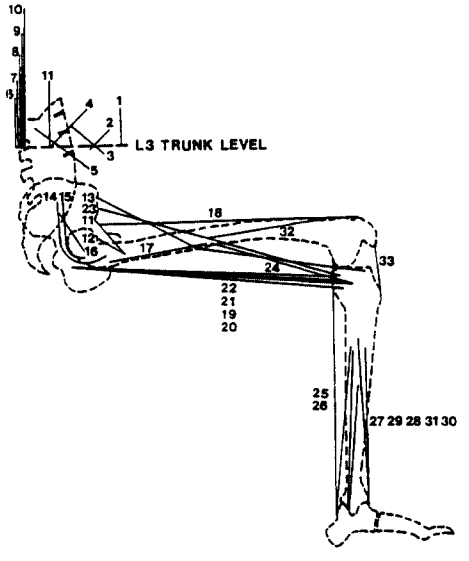


**Fig. 3** Schematic representation of trunk and lower extremity model with single muscle equivalents on the right side of the body. These represent RAB (1) ; medial internal oblique, MIO (2) ; MEO (3) ; lateral internal oblique, LIO (4) ; lateral external oblique, LEO (5) ; latissimus, LAT (6) ; MUL (7) ; longissimus, LON (8) ; iliocostalis, COS (9) ; quadratus, QUD (10) ; PSO (11) ; CUS (12) ; TFL (13) ; GMA (14) ; GME (15) ; PIR (16) ; ADD (17) ; RFM (18) ; BFL (19) ; SMM (20) ; STN(21) ; GRA (22) ; SAR (23) ; BFS (24) ; GAM (25) ; GAL (26) ; SOL (27) ; TPO (28) ; PER (29) ; TAN(30) ; EDL (31) ; QUA (32) ; and PAT (33). See text for abbreviations.

latae (TFL), single muscle equivalent of gluteus maximi (GMA), single muscle equivalent of posterior and medial portions of gluteus medii (GME), piriformis (PIR), adductor longus (ADD), rectus femoris (RFM), biceps femoris longus (BFL), gracilis (GRA), sartorius (SAR), semimembranosus (SMM), and semitendinosus (STN) on either side. The single equivalent muscles at the knee joint were tensor fasciae latae (TFL), patellar tendon (PAT), biceps femoris longus (BFL), semimembranosus (SMM), semitendinosus (STN), gracilis (GRA), sartorius (SAR), biceps femoris short head (BFS), gastrocnemius medialis (GAM), and gastrocnemius lateralis (GAL). The single equivalent muscles modelled at the ankle joint were gastrocnemius medialis (GAM), gastrocnemius lateralis (GAL), soleus (SOL), tibialis posterior (TPO), peroneus longus (PER), tibialis anterior (TAN), and extensor digitorum longus (EDL).

### 2.4 Linear optimization schemes

Let n be the number of muscles modelled ; k the number of joints modelled ; m the number of moment components to be modified by passive tissue resistance ; $a_{ij}$ the moment arm component of the $j$-th muscle for the $i$-th moment component ($b_i$) due to solely active muscle contractions ; $c_{lj}$ the moment arm component of the $j$-th muscle for the $l$-th moment component ($d_l$) due to combined effects of muscle contractions and passive resistance ; $g_j$ the cross-sectional area of the $j$-th muscle ; and $h_j$ the coefficients to be assigned to the $j$-th muscle for an objective function. With these known parameters of the musculoskeletal system, the problem can be formulated for unknown $j$-th muscle force ($x_j$) and resultant muscle stress ($S$) :

$$\text{minimize}\{h_0 S + \sum_{j=1}^{n} h_j x_j\}, \tag{1}$$

subject to :

$$\sum_{j=1}^{n} a_{ij} x_j = b_i \qquad i=1, 2, \cdots, (3\text{k-m}), \tag{2}$$

$$\sum_{j=1}^{n} c_{lj} x_j \leq d_l \qquad l=1, 2, \cdots, 2\,\text{m}, \tag{3}$$

$$x_j / g_j \leq S \qquad j=1, 2, \cdots, \text{n}, \tag{4}$$

$$x_j \geq 0 \qquad j=1, 2, \cdots, \text{n}. \tag{5}$$

This study used the double linear programming method (DLPM) published by Bean et al.(1988) : firstly, the value of muscle stress $S$ was minimized by putting $h_0=1$ and $h_j=0$ for $j \geq 1$ in (1) while expressions (2), (3), and (5) were satisfied ; secondly, muscle forces were obtained which minimized objective function (1) (see below) while expressions (2), (3), (4), and (5) were satisfied.

For comparison purpose, four different objective functions A, B, C, and D were used in the second solution step of DLPM. They depended on the coefficients in (1). The value of $h_0$ was zero in every case, but a set of values of $h_j$ for $j \geq 1$ was distinct in each objective function. The coeffi-

cients were for $j \geq 1$ : (A) $h_j = 1$ which minimized the sum of muscle forces, (B) $h_j = 1/g_j$ which minimized the sum of muscle stresses, (C) $h_j = 100$ if the $j$-th muscle crosses the hip joint and $h_j = 1$ otherwise, which put a heavier (100 times) penalty on use of muscles crossing the hip joint, (D) $h_j = l_{jz}$, where $l_{jz}$ $(-1 \leq l_{jz} \leq 1)$ is the direction cosine of the line-of-action of the $j$-th muscle to the $z$-axis of the global coordinate system, which minimized the sum of all lateral joint force components exerted by muscles. These four optimization schemes were selected from the most promising of 12 candidate schemes studied in Son(1988) using a quantitative evaluation of the muscle force predictions (Son, 1990).

Solution sets were found to be dependent upon how the contraction force in a two-joint muscle was calculated at its proximal and distal joints (Son, 1988 ; Son and Miller, 1988). The reason for this is that, when two-joint muscles are modelled in a multi-joint system, the stepwise treatment of each joint makes a multi-joint system with two-joint muscles equivalent to a system with multiple isolated single joints. In this study the efficacy of the above four global schemes and a local scheme was examined. The local scheme involved stepwise calculation of one- and two-joint muscle forces acting about the ankle, then the knee, then the hip joints, and finally the trunk. Since this scheme was found to provide the same solution set regardless of different objective functions used in the second step of DLPM, it was denoted by Scheme E for comparison purposes.

### 2.5 Correlation method

The linear correlation coefficient ($r$) between the predicted and measured muscle activity was calculated over a one second time period (Son and Miller, 1988 ; Son, 1990). For each of the 15 muscles from which EMG signals were monitored, the correlation was based on the 31 pairs of sequential data points representing predicted force and measured EMG. Then, the number of muscles ($N_{sig}$) whose $r$'s reached statistical significance was used as a quantitative measure of ranking the efficacy of the different prediction schemes.

## 3. Results

### 3.1 Joint moments during the four tasks

Joint moments were calculated for each task where a hand-held weight was moved in the sagittal plane. Figs. 4(a) through 4(d) show time histories of the moment components acting at the third lumbar (L3) of the trunk, and the right and left hip, knee, and ankle joints for a subject (Subject RC) for a single cycle of each of the four tasks. In each figure, one horizontal axis denotes 21 moment components at the seven joints, the other horizontal axis denotes 31 time steps during a task cycle, the vertical axis denotes moment magnitude, and approximate arm positions during task performance were shown next to the time axis.

The moment-time pattern was closely related to the anterior-posterior arm segment position and movement pattern, as expected. Not surprisingly, the variation in the $z$-component (flexion-extension moment component) was greatest at the L3 level, diminishing as one moved distally to knee and ankle joints. Thus, the trunk and hip moments were found to be quite sensitive to task type, while the knee and ankle joint moments were less sensitive.

Noticeable intertask differences in joint moments were found from Figs. 4(a) through 4(d). The flexion-extension moments reached 65, 42, 49, and 32 Nm at the L3 trunk ; 20, 14, 14, and 8 Nm at the right hip joint ; 21, 15, 28, and 10 Nm at the left hip joint ; 5, 3, 6, and 4 Nm at the right knee joint ; 5, 3, 7, and 4 Nm at the left knee joint ; 11, 13, 11, and 9 Nm at the right ankle joint ; 14, 6, 14, and 8 Nm at the left ankle joint in Tasks 1, 2, 3, and 4, respectively. A considerable ($>16$ Nm) difference in the maximum trunk moment between the two-handed task (Task 1) and the right-handed tasks (Tasks 2, 3, and 4) clearly showed the effect of the inertial and gravitational forces of the left arm segments and the additional weight of 1kg mass. An asymmetric use of lower extremities for body equilibrium was also found from joint moment values in the two-handed symmetric task as well as in the right-handed

tasks. The right-left moment difference was largest (14 Nm) at the hip joint in the right-handed arm-stretching task (Task 3), while it was negligible at the knee joint in all four tasks. A comparison of the maximum values of ankle joint moment revealed an ironical fact that the symmetric task had a larger (3 Nm) difference than the right-handed arm-folding task (Task 4) had.

For the seven subjects, the joint flexion moments are summarized in terms of the mean values and standard deviations (Table 1). A negative value of the mean joint moment indicates that an extension moment was exerted at that joint. Intersubject variations in extremum joint moment values were so large that the coefficient of variation (CV) exceeded 0.3 at each joint for all four tasks. The CV's reached up to 1.3, 37.0, 1.0, and 0.6 at the trunk, hip, knee, and ankle joints, respectively. The main reasons for these large CV's could be personal differences in anthropometry, weight-moving stroke, and feet or hip supporting strategy. It was also found that, con-

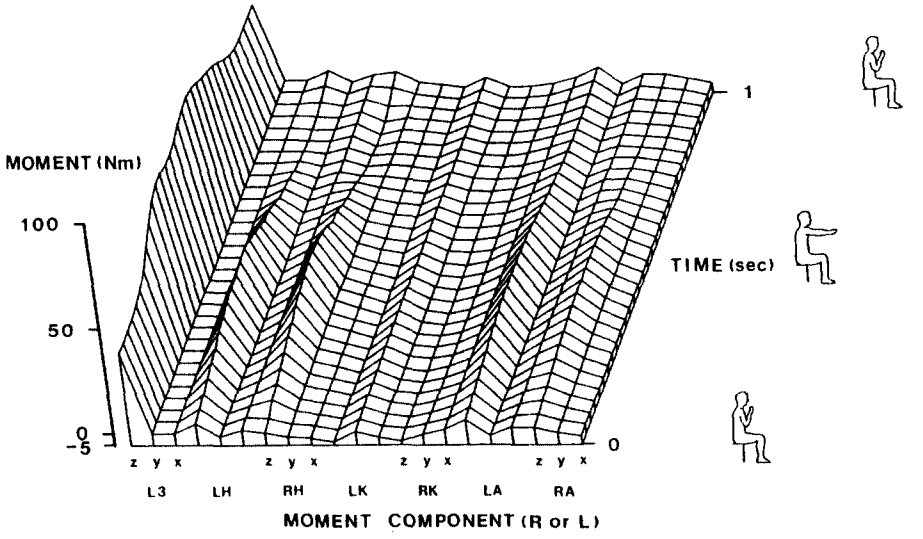


(a) Two-handed cyclic task (Task 1)

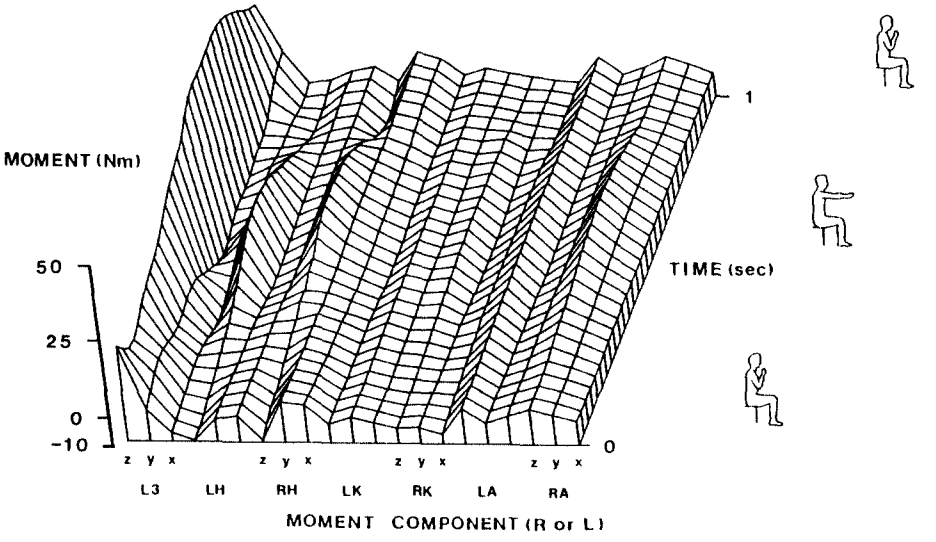


(b) Right-handed cyclic task (Task 2)

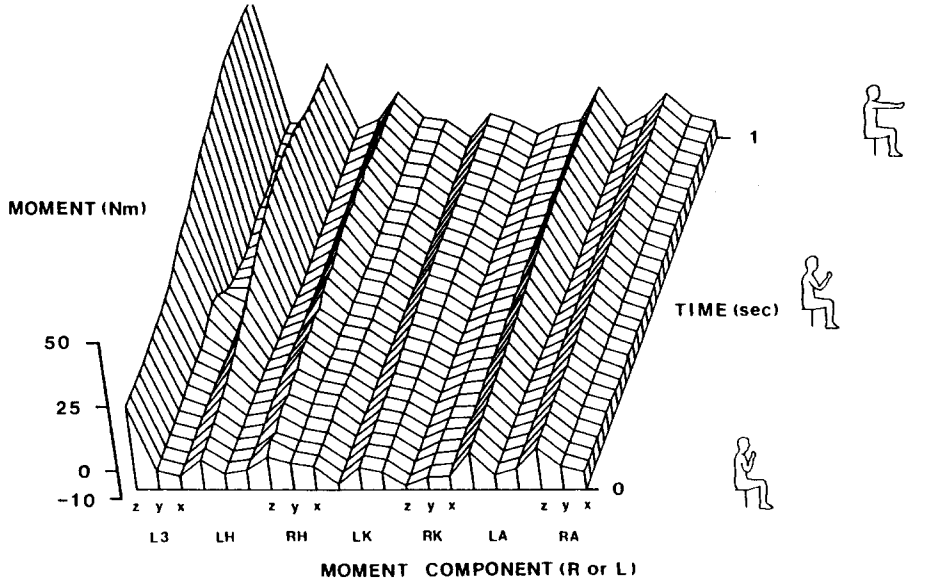


(c) Right-handed stretching task (Task 3)

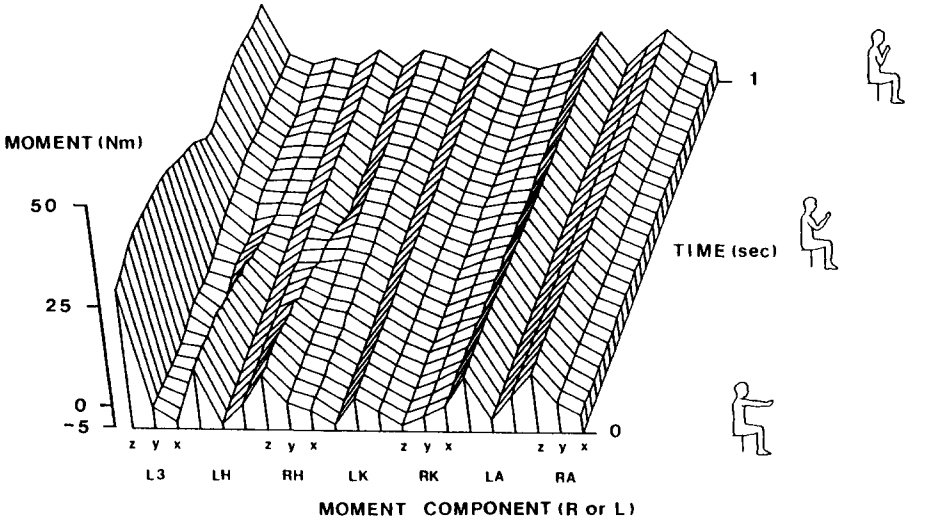


(d) Right-handed folding task (Task 4)

**Fig. 4** Time histories of moment components at the trunk and lower extremity joints in four tasks by Subject RC

sidering both sides of the body, the hip joint moment reached the magnitude of the trunk moment and the ankle joint moment reached more than a half of that for all tasks.

### 3.2 Muscle force predictions

Determination of passive moments : The three passive moments considered were the knee varus-valgus rotational moment (PM 1), the knee internal-external rotational moment (PM 2), and the ankle internal-external rotational moment (PM 3). Since no data on the average passive moments are available for the seated position, ranges of plausible values were taken from the available literature. Then the "appropriate" combination of passive moments was determined by a sensitivity analysis, changing one variable at a

**Table 1** The mean and standard deviation (SD) of the extremum values of the flexion moments at the L3 trunk, right (R) and left (L) hip joints (H.J.), knee joints (K.J.), and ankle joints (A.J.) for the seven subjects during each task cycle

| Joint | | Flexion Moment (Nm) | | | | | | | |
|---|---|---|---|---|---|---|---|---|---|
| | | Task 1 | | Task 2 | | Task 3 | | Task 4 | |
| | | Min | Max | Min | Max | Min | Max | Min | Max |
| L3 Trunk | Mean | 10.5 | 44.0 | 7.7 | 27.9 | 13.5 | 29.9 | 5.2 | 22.4 |
| | SD | 13.7 | 14.9 | 5.5 | 8.4 | 6.3 | 11.0 | 5.5 | 6.0 |
| H.J. (R) | Mean | -5.2 | 21.0 | 0.2 | 10.9 | 2.6 | 11.2 | -3.6 | 6.8 |
| | SD | 5.5 | 8.7 | 7.4 | 3.5 | 6.7 | 7.5 | 5.7 | 5.2 |
| H.J. (L) | Mean | -4.6 | 19.8 | -1.5 | 19.0 | 2.9 | 17.3 | -2.8 | 9.2 |
| | SD | 8.7 | 5.5 | 5.5 | 4.8 | 6.7 | 9.9 | 8.0 | 7.9 |
| K.J. (R) | Mean | -5.4 | -2.2 | -5.5 | -3.3 | -5.8 | -4.0 | -4.9 | -3.2 |
| | SD | 2.9 | 2.0 | 2.0 | 2.7 | 1.8 | 1.4 | 1.6 | 1.3 |
| K.J. (L) | Mean | -6.3 | -2.9 | -6.1 | -2.7 | -7.0 | -4.7 | -5.9 | -3.5 |
| | SD | 2.7 | 2.9 | 2.4 | 1.9 | 2.0 | 1.8 | 2.1 | 1.6 |
| A.J. (R) | Mean | 3.3 | 10.3 | 4.9 | 9.8 | 5.5 | 8.1 | 5.2 | 7.4 |
| | SD | 1.6 | 4.2 | 1.8 | 2.5 | 3.3 | 3.4 | 1.8 | 2.5 |
| A.J. (L) | Mean | 4.2 | 11.9 | 5.3 | 8.9 | 5.8 | 9.1 | 5.7 | 7.4 |
| | SD | 2.5 | 4.0 | 2.6 | 3.3 | 3.1 | 3.8 | 2.8 | 3.2 |

time.

The sensitivity analysis was based on a single subject (Subject GW) in a single task (Task 1). An allowable muscle stress is bounded by a physiological limit, therefore, the resultant muscle stress was used as a criteria to judge the acceptability of passive moment values. We started the sensitivity analysis with values of 5.0, 0.02, and 0.3 Nm (Andriacchi et al., 1983 ; Gottlieb and Agarwal, 1978) for PM's 1, 2, and 3, respectively. It was found that individual muscle stress was most sensitive to change in PM 3 so that an increase in PM 3 from 0.3 to 2.0 Nm caused a reduction in muscle stress approximately to half for most muscles (Son, 1988). This value of PM 3 was taken, and then all the muscle force predictions were made using 5.0, 0.02, and 2.0 Nm for PM's 1, 2, and 3, respectively.

Muscle force predictions by different optimization schemes : Figs. 5(a) through 5(e) show time histories of muscle forces which were predicted using the five different optimization schemes A, B, C, D, and E for a given subject (Subject RC) performing the right-handed folding task (Task 4). These five figures show the predicted forces in the 32 right side muscle equivalents at each time step of a single task cycle. The predicted left side muscle forces using Scheme A are shown in Fig. 5(f) in order to investigate the right-left difference in muscle forces for Task 4. In most figures, the predicted muscle forces in trunk extensors (for example, COS, QUA, and PSO) clearly indicate the posterior arm segment movement during this task.

Fig. 5(a) shows predicted muscle forces when the sum of muscle forces was minimized at the second step of the double linear programming method (DLPM). Higher forces ( $>100$ N in their maximum values) were predicted in such muscles as LON, COS, PSO, GMA, ADD, and GAM. For convenience, this prediction was taken as the reference in comparing with the other predictions.

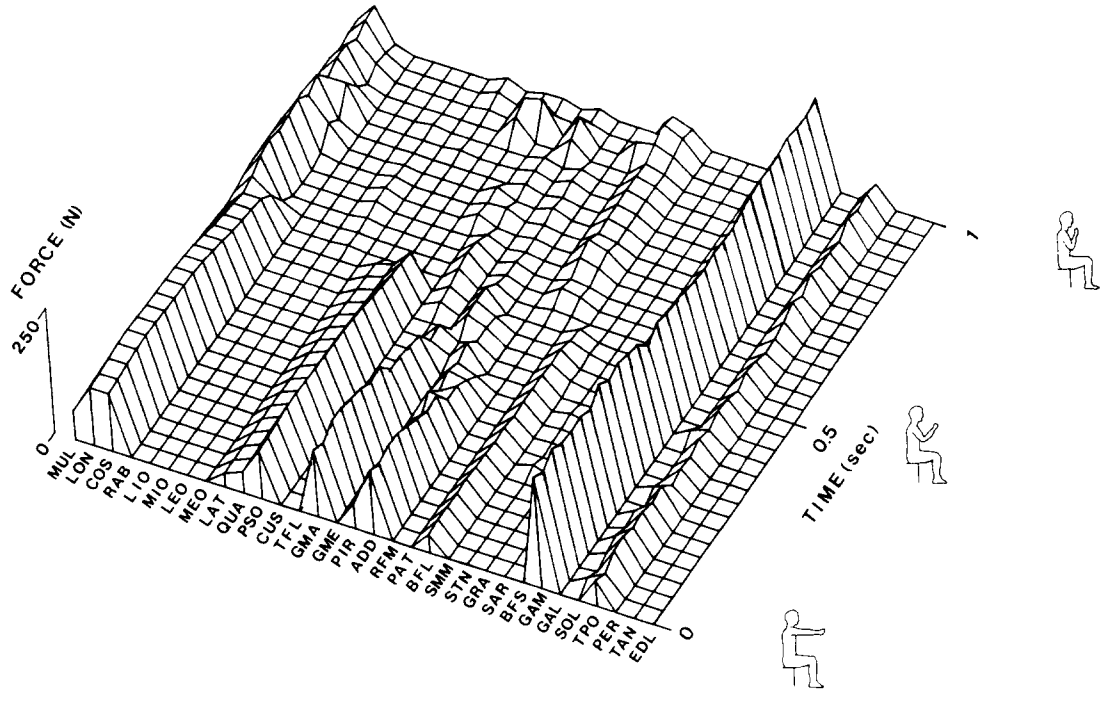


(a) Scheme A

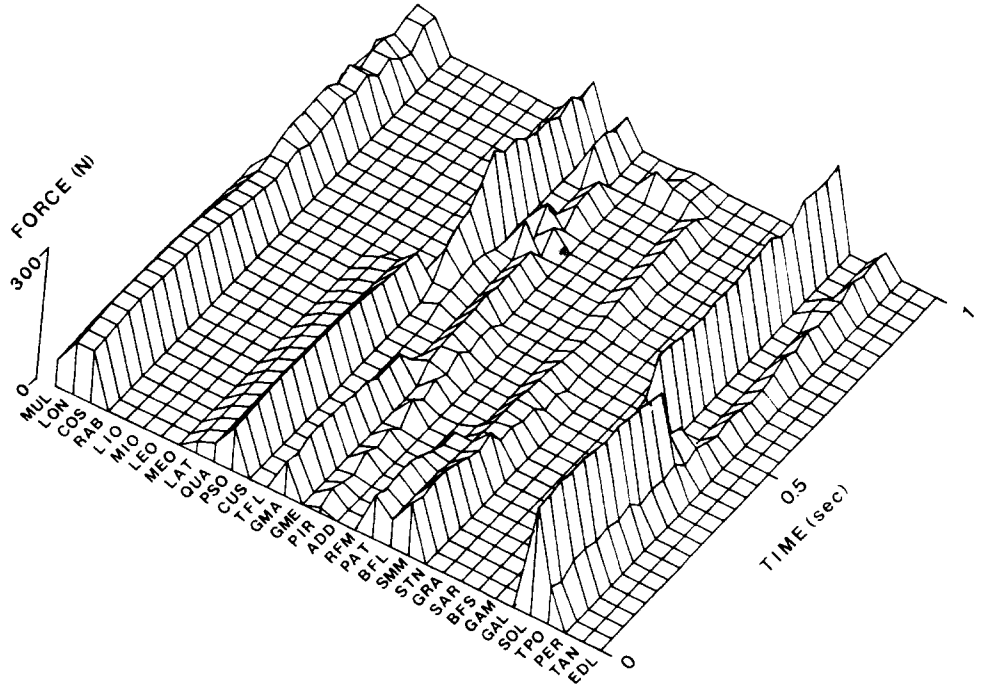


(b) Scheme B

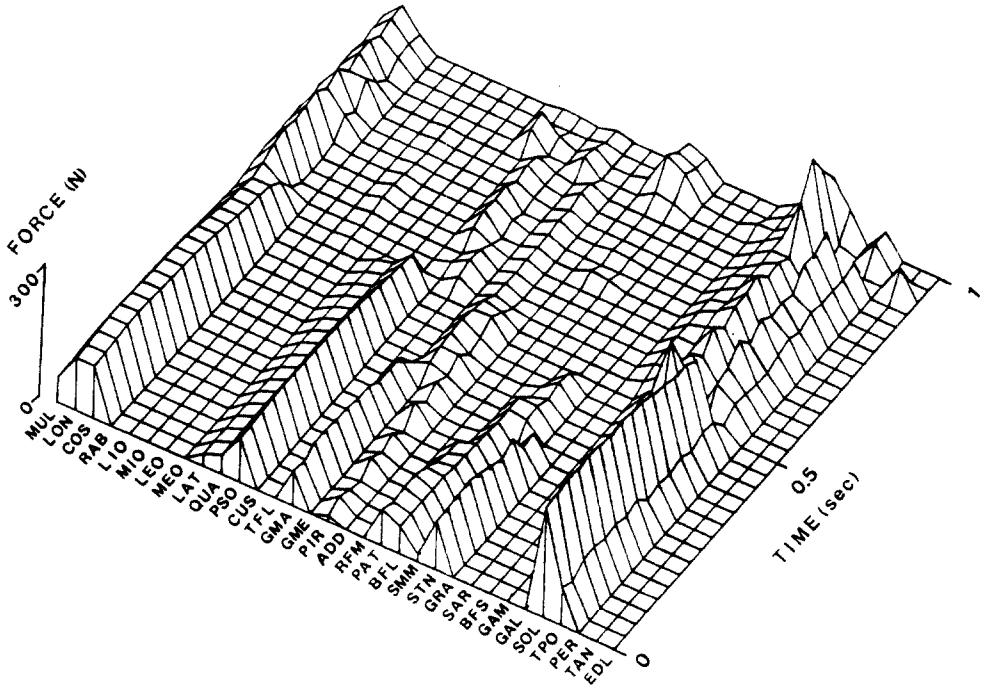


(c) Scheme C

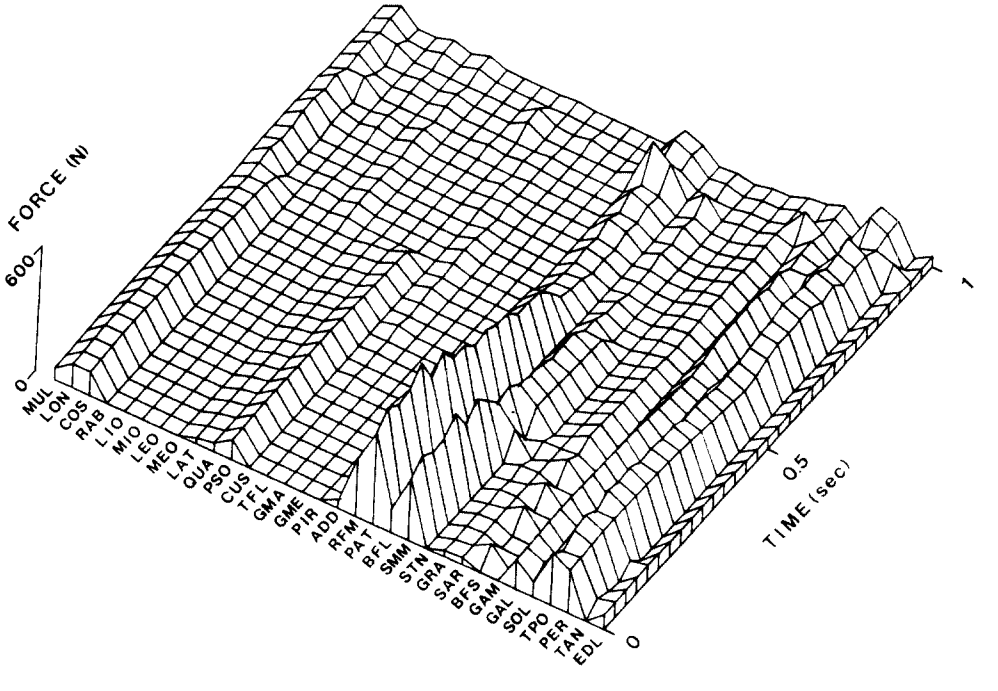


(d) Scheme D

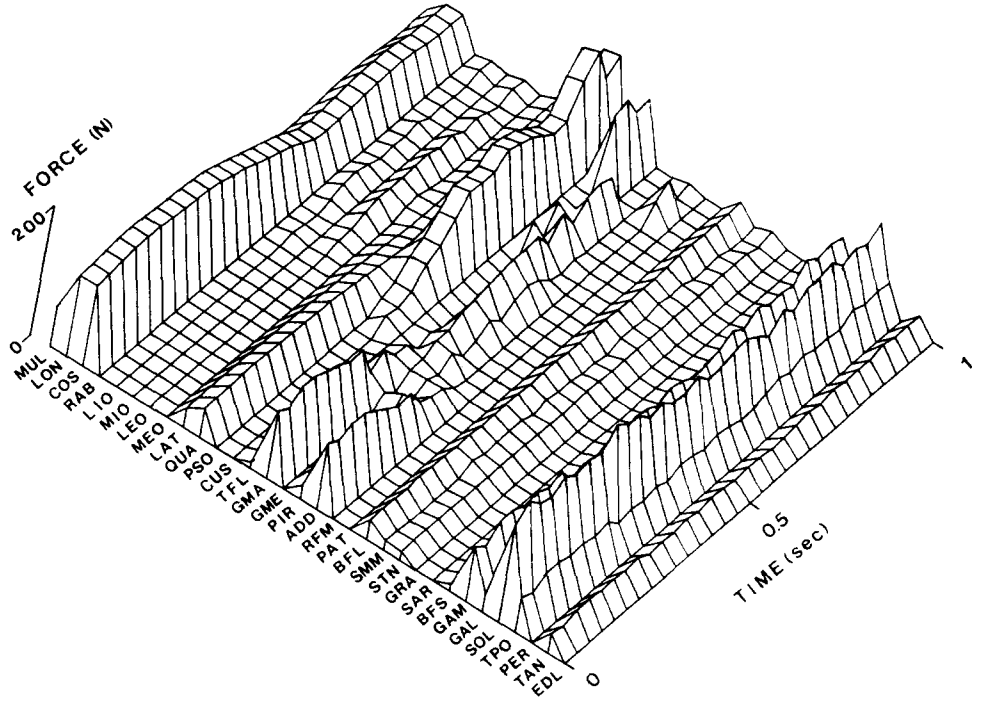


(e) Scheme E

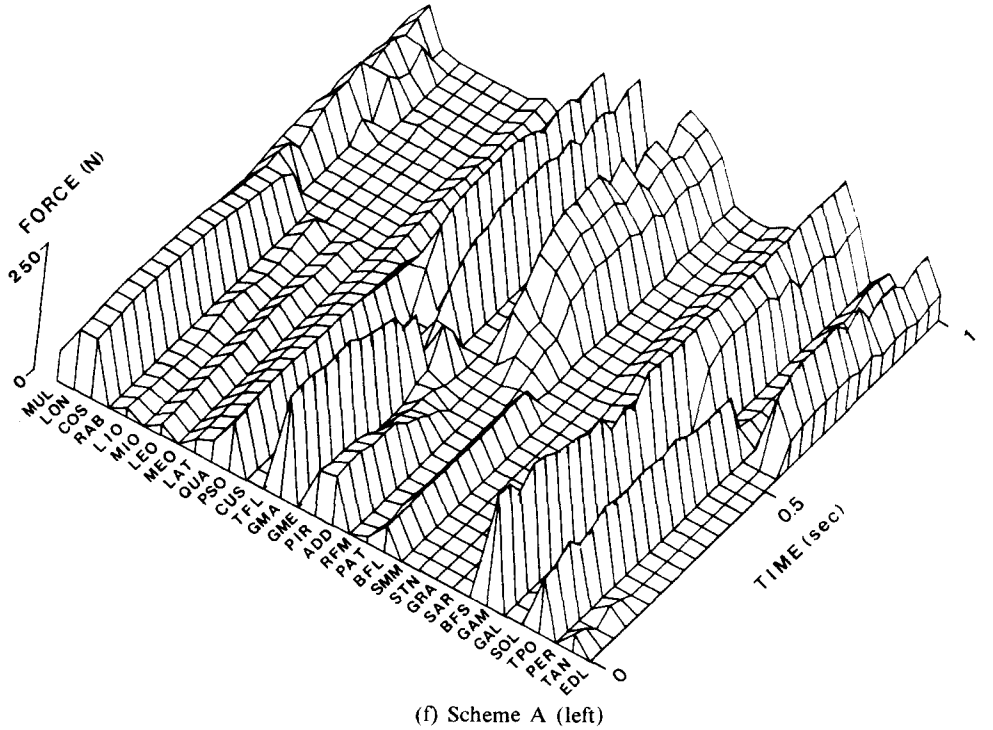


(f) Scheme A (left)

**Fig. 5** Predicted forces in the trunk and lower extremity muscles (a, b, c, d, and e for the right side; f for the left side) of Subject RC during Task 4 using different schemes

When the minimal muscle stress was used as an objective function (Fig. 5(b)), such lower extremity muscles as CUS, PAT, SMM, and SOL whose PCSA are relatively larger ($>15$ cm$^2$) were predicted to carry increased forces in comparison with Fig. 5(a). It should be noted that ankle flexors (GAM and SOL) were predicted to switch their major activity for different arm positions: SOL reached the highest muscle force (250 N) when the right arm was extended and GAM reached the highest (180 N) when the right arm was flexed. This was probably caused by the interrelation of the triceps surae, the synergistic plantar-flexors, for three-dimensional moment equilibrium at the ankle joint.

When the hip joint force was penalized by 100 times more than the other joint forces (Fig. 5(c), the one-joint muscles around the hip joint (CUS, GMA, GME, PIR, and ADD) were predicted to carry reduced forces than those in Fig. 5(a). This made the two-joint muscles (RFM, BFL, SMM, and STN) crossing the hip and knee joints carry up to 175 N for hip joint equilibrium. For knee joint equilibrium, on the other hand, the activity of GAM was predicted to be negligible when the right arm was extended. This made SOL (one-joint plantarflexor) carry an increased force up to 250 N contrary to Fig. 5(a). Almost no change was found in trunk muscle forces when compared with predictions using Scheme A.

When the sum of the lateral component of the joint forces was minimized (Fig. 5(d), the muscles whose lateral lever arm are negligible were predicted to carry extremely large forces ($>360$ N) as in RFM, PAT, and SMM. This made, in turn, one-joint hip muscles carry noticeably reduced forces. Another prominent finding was that the most of the knee and ankle muscles were predicted to have non-zero muscle forces when compared with the previous cases. Furthermore, all the ankle muscles were predicted to carry considerably large forces ranging from 80 to 260 N in their maximum values.

When muscle forces were determined joint by joint from ankle joint, then proximally up to L3 trunk (Fig. 5(e), each different objective function at the second step of DLPM resulted in the same muscle forces; this is a similar result to that found by Son and Miller(1988). It should be noted that both LON and COS had a muscle force-time pattern quite similar to the moment-time pattern of the trunk flexion-extension component (see Fig. 4(d). Higher forces ($>100$ N) were predicted mostly in one-joint muscles such as LON, COS, CUS, GMA, ADD, and SOL.

The predicted forces in left side lower extremity muscles as shown in Fig. 5(f) look noticeably different in overall activity patterns from those in the right side (Fig. 5(a) especially when the arm was being folded and flexed (after $t = 0.5$ second). This result was entirely due to slight right-left differences in three-dimensional moment components (see Fig. 4(d), for the same scheme was used. This finding indicates that the muscle forces predicted using a linear optimization scheme turned out to be very sensitive to the joint loading.

The most successful prediction schemes for different tasks: A quantitative comparison between the predicted and measured muscle activities was achieved using the linear correlation coefficients ($r$'s). As an example, these correlation coefficients for a subject (Subject RC) performing the right-handed arm-folding task (Task 4) were given in Fig. 6 with the time histories of the predicted muscle forces and measured EMG data which were normalized by their maximum values. The $t$-distribution, based on the 31 data points for each muscle, yielded the $r$ value statistically significant for a 95% confidence interval ($p<0.05$) when $r>0.36$. As a way of ranking the five different prediction schemes, the "best" scheme was selected as the one resulting in the largest number of statistically significant correlation coefficients $N_{sig}(r>0.36)$.

Based on the value of $N_{sig}$, the selected best scheme was listed in Table 2. The case when no feasible solution was found at one or more time steps was indicated by - in the table, whereas $N_{sig}$ was filled in the parentheses. The minimal lateral joint force criterion (Scheme D) was the most successful in predicting muscle forces for Tasks 1 and 4, while the local scheme (Scheme E) was so for Task 2 and the minimal stress criterion (Scheme B) was so for Task 3. It should be noted

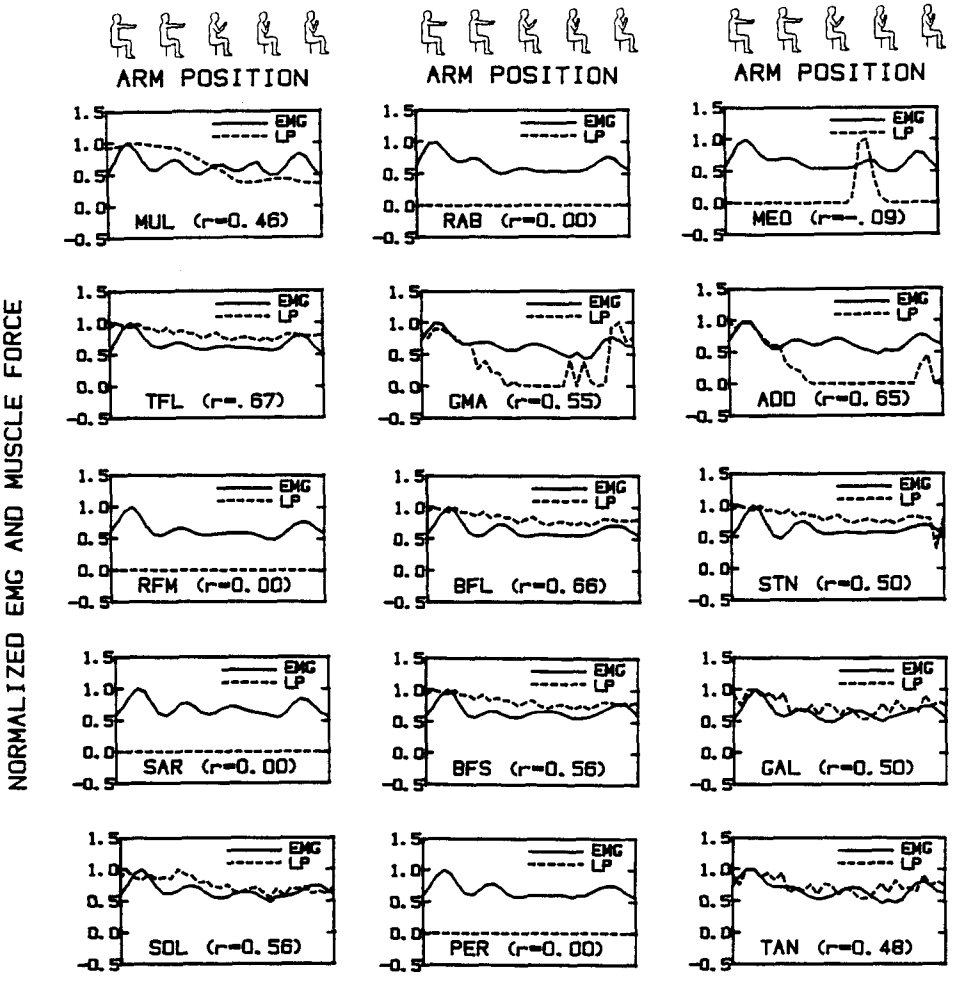


**Fig. 6** Predicted forces and measured EMG data for 15 trunk and lower extremity muscles of Subject RC during Task 4

**Table 2** Most successful solutions for muscle activity prediction based on $N_{sig}$

| Task | Subject | | | | | | |
|---|---|---|---|---|---|---|---|
| | LJ | JM | RC | NC | MT | GW | JE |
| Task 1 | E(6) | A(5) | B(4) | D(9) | E(7) | D(7) | C(6) |
| Task 2 | E(6) | A(3) | E(9) | - | D(8) | - | - |
| Task 3 | - | C(5) | B(3) | - | - | A(3) | B(6) |
| Task 4 | - | D(4) | E(10) | - | A(6) | - | D(5) |

that no one prediction scheme exceeded the majority of 19 cases. It was interesting that the best prediction scheme was not the same for a given subject performing the four different tasks. This was also true for the other subjects. Another important finding was that the best prediction scheme was not the same for all the subjects in each of the four tasks.

## 4. Discussion

To date, no study has quantified the efficacy of an objective function in the same subject performing different tasks. To facilitate comparisons we purposefully selected all tasks to be sub-maximal in nature, all to involve sagittal plane movements of the upper extremities, the only difference being whether one or both upper extremities were used and whether tasks were uni-directional or cyclic. One important finding in this study was that no single objective function emerged as "best" for a given subject in all four tasks. We also found that the best prediction scheme was not the same for all subjects performing any of the four tasks, supporting a similar finding in our earlier two-dimensional analysis of the two-handed cyclic task (Son and Miller, 1988).

Which objective function was the most successful for all 19 cases? In short, although Scheme D (minimization of the sum of the lateral components of joint forces) and Scheme E (local scheme) are candidates because $N_{sig}$ ranged from 6 to 10 in five cases of Scheme E and $N_{sig}$ ranged from 4 to 9 in five cases of Scheme D, neither scheme was particularly successful over all cases.

$N_{sig}$ ranged from 3 to 10 for all 19 cases (Table 2) ; is this value satisfactory? The low $N_{sig}$ value was partly associated with the use of a linear objective function. Hardt(1978) indicated that a linear constraint space with a linear objective function limits the number of nonzero variables in a basic feasible solution. Thus, using a linear objective function implicitly avoided predicting simultaneous activity of agonistic and antagonistic muscles at a joint, while co-contractions were clearly observed especially in the trunk and ankle muscles for most subjects. The prediction based on minimal co-contractions made some muscles carry no force at every time step. Figure 6 shows typical examples of the null-predicted muscle force, i.e. $r=0.00$, in four muscles (RAB, RFM, SAR, and PER). The number of these muscles is listed in Table 3 for each of the 19 cases in Table 2. The number of muscles with $r=0.00$ ranged 1 to 10 with an average value of 4 ($>25\%$ of the 15 muscles correlated). This number would be possibly decreased in case of using a nonlinear objective function. Nevertheless, it would not be guaranteed that this case is free of a zero correlation coefficient. Since the muscles with zero correlation coefficients took a considerable portion of the whole set of the 15 muscles and their EMG signals can never be zero at all time steps due to inherent noise, these muscles had to be evaluated in a different way depending on their maximum EMG magnitudes. It would be a way to define the "lack" of muscle activity as being less than a certain threshold. However, this consideration requires more studies of the "appropriate" EMG threshold for the fully relaxed state of a muscle. Therefore, the seemingly low value of $N_{sig}$ is not so discouraging when counting the number of muscles with zero correlation coefficients.

Did this three-dimensional model, with its superior representations of the musculature, more muscles and capabilities for taking asymmetric joint loading into account, yield better results for the symmetric task than its two-dimensional counterpart (Son and Miller, 1988)? Based on the values of $N_{sig}$ our results suggest not. For joint

**Table 3** Number of muscles whose activities were predicted to be null at every time step by each optimization scheme listed in Table 2

| Task | Subject | | | | | | |
|---|---|---|---|---|---|---|---|
| | LJ | JM | RC | NC | MT | GW | JE |
| Task 1 | 3 | 2 | 4 | 3 | 4 | 1 | 4 |
| Task 2 | 2 | 6 | 2 | - | 5 | - | - |
| Task 3 | - | 4 | 10 | - | - | 6 | 5 |
| Task 4 | - | 3 | 4 | - | 4 | - | 6 |

flexion-extension moments, the two-dimensional model covered most of the functionally important muscles. Because we tried to keep the number of muscles to a minimum for computational and economic reasons, the limited number of model muscles, particularly about the knee joints, sometimes prevented a feasible solution set for the prediction of lower extremity muscle forces (see Table 2). A larger model with all the lower extremity muscles (47 muscles on each side) might solve this problem and produce a distinct solution set for each objective function in the sequential local procedure, but at a considerably greater computational cost and with no guarantee of success.

Moments due to passive stiffness properties were added to the knee and ankle joints in order to supply the portion of moment exerted by neglected muscles, ligaments, and other passive elements around those joints. It is well known that passive stiffness is a function of such variables as the position of lower limb elements and loading conditions (Piziali et al., 1977 ; Gottlieb and Agarwal, 1978 ; Andriacchi et al., 1983 ; Siegler et al, 1984 ; Shoemaker and Markolf, 1985 ; Mansour and Audu, 1986 ; Louie and Mote, 1987). Since passive joint data for lower extremity joints in the seated position were unavailable, we had to rely upon incomplete published data, necessitating some "educated guesses" and a sensitivity analysis. We might have obtained improved results if more reliable data had been available.

These findings show that the main factors influencing the success of muscle force predictions were the specific three-dimensional joint loading, the particular muscles modelled around each joint, the passive stiffness properties of a joint, and the prediction scheme. At the ankle joint, for example, a particular loading vector might easily be equilibrated by the seven model muscles (GAM, GAL, SOL, TPO, PER, TAN, and EDL)-yielding a "good" prediction (high $r$ values). If a loading vector was such that neglected muscles (extensor hallucis, flexor digitorum, flexor hallucis, peroneus brevis, and peroneus tertius) are really required for ankle equilibrium, then a "poor" prediction could result for the modelled muscles which now, in addition, have to substitute for those neglected muscles. To a certain extent, the absence of the neglected muscles can be compensated for by adding the passive joint moment in certain directions. However, even with the addition of passive joint moments no feasible solution was found in some cases (see Table 2). Under yet another loading vector, the modelled muscles may be oriented such that only one combination of muscle forces is capable of establishing equilibrium. So, the solution may be "good" or "bad" depending on subtle changes in a loading vector. Changes in loading vector can result from slightly different arm segment accelerations, or subtle differences in the way the foot is used.

## 5. Conclusions

This study provided a theoretical basis for a broader understanding of the mechanical requirements of the seated position. This can lead to advances in clinical applications and treatments, and improved ergonomic designs. The results showed that the most successful linear objective function was not the same for all subjects performing a given task or a given subject performing all four tasks. The efficacy of an objective function was found to be critically dependent upon details of joint loading, joint passive stiffness properties, and postural control strategy. The model adequately predicted the time history of muscle activity in up to two-thirds of the 15 unilateral muscles whose EMG signals were measured, when judged by the number of statistically significant correlation coefficients. Thus linear objective functions seem to be useful tools in predicting muscle forces.

## References

An, K.N., Kwak, B.M., Chao, E.Y. and Morrey, B.F., 1984, "Determination of Muscle and Joint Forces : A New Technique to Solve the Indeterminate Problem," ASME J. Biomech. Eng., Vol. 106(4), pp. 364~367.

Andersson, G.B.J., 1974, "On Myoelectric Back

Muscle Activity and Lumbar Disc Pressure in Sitting Postures," Ph.D. Dissertation, Univ. of Göteborg, Göteborg, Sweden.

Andersson, G.B.J., Örtengren, R. and Schultz, A., 1980, "Analysis and Measurements of the Loads on the Lumbar Spine during Work at a Table," J. Biomechanics, Vol. 13(6), pp. 513 ~520.

Andriacchi, T.P., Mikosz, R.P., Hampton, S.J. and Galante, J.O., 1983, "Model Studies of the Stiffness Characteristics of the Human Knee Joint," J. Biomechanics, Vol. 16(1), pp. 23~29.

Bader, D.L. and Hawken, M.B., 1986, "Pressure Distribution under the Ischium of Normal Subjects," J. Biomed. Eng., Vol. 8, pp. 353~357.

Bean, J.C., Chaffin, D.B. and Schultz, A.B., 1988, "Biomechanical Model Calculation of Muscle Contraction Forces : A Double Linear Programming Method," J. Biomechanics, Vol. 21(1), pp. 59~66.

Bendix, T., 1984, "Seated Trunk Posture at Various Seat Inclinations, Seat Heights, and Table Heights," Human Factors, Vol. 26(6), pp. 695~703.

Brand, R.A., Pedersen, D.R. and Friederich, J. A., 1986, "The Sensitivity of Muscle Force Predictions to Changes in Physiologic Cross-Sectional Area," J. Biomechanics, Vol. 19(8), pp. 589~596.

Crowninshield, R.D., 1978, "Use of Optimization Techniques to Predict Muscle Forces," ASME J. Biomech. Eng., Vol. 100(2), pp. 88~92.

Crowninshield, R.D. and Brand, R.A., 1981, "A Physiologically Based Criterion of Muscle Force Prediction in Locomotion," J. Biomechanics, Vol. 14(11), pp. 793~801.

Davy, D.T. and Audu, M.L., 1987, "A Dynamic Optimization Technique for Predicting Muscle Forces in the Swing Phase of Gait," J. Biomechanics, Vol. 20(2), pp. 187~201.

Gottlieb, G.L. and Agarwal, G.C., 1978, "Dependence of Human Ankle Compliance on Joint Angle," J. Biomechanics, Vol. 11(4), pp. 177 ~181.

Hardt, D.E., 1978, "Determining Muscle Forces in the Leg during Normal Human Walking-An Application and Evaluation of Optimization Methods," ASME J. Biomech. Eng., Vol. 100(2), pp. 72~78.

Knutsson, B., Lindh, K., and Telhag, H., 1966, "Sitting-An Electromyographic and Mechanical Study," Acta. Orthop. Scandinav., Vol. 37, pp. 415~428.

Louie, J.K. and Mote Jr., C.D., 1987, "Contribution of the Musculature to Rotatory Laxity and Torsional Stiffness at the Knee," J. Biomechanics, Vol. 20(3), pp. 281~300.

Mansour, J.M. and Audu, M.L., 1986, "The Passive Elastic Moment at the Knee and Its Influence on Human Gait," J. Biomechanics, Vol. 19(5), pp. 369~373.

McConville, J.T., Churchill, T.D., Kaleps, I., Clauser, C.E. and Cuzzi, J., 1980, "Anthropometric Relationships of Body and Body Segment Moments of Inertia," AFAMRL-TR-80-119, Aerospace Medical Research Laboratory, Wright-Patterson Air Force Base, Ohio.

Németh, G. and Ohlsén, H., 1985, "In Vivo Moment Arm Lengths for Hip Extensor Muscles at Different Angles of Hip Flexion," J. Biomechanics, Vol. 18(2), pp. 129~140.

Occhipinti, E., Colombini, D., Frigo, C., Pedotti, A. and Grieco, A., 1985, "Sitting Posture : Analysis of Lumbar Stresses with Upper Limbs Supported," Ergonomics, Vol. 28(9), pp. 1333~1346.

Patriarco, A.G., Mann, R.W., Simon, S.R. and Mansour, J.M., 1981, "An Evaluation of the Approaches of Optimization Models in the Prediction of Muscle Forces during Human Gait," J. Biomechanics, Vol. 14(8), pp. 513~525.

Pedotti, A., Krishnan, V.V. and Stark, L., 1978, "Optimization of Muscle-Force Sequencing in Human Locomotion," Math. Biosci., Vol. 38, pp. 57~76.

Penrod, D.D., Davy, D.T. and Singh, D.P., 1974, "An Optimization Approach to Tendon Force Analysis," J. Biomechanics, Vol. 7(2), pp. 123~129.

Piziali, R.L., Rastegar, J.C. and Nagel, D.A., 1977, "Measurement of the Nonlinear, Coupled Stiffness Characteristics of the Human Knee," J. Biomechanics, Vol. 10(1), pp. 45~51.

Röhrle, H., Scholten, R., Sigolotto, C., Sollbach, W. and Kellner, H., 1984, "Joint Forces in

the Human Pelvis-Leg Skeleton during Walking," J. Biomechanics, Vol. 17(6), pp. 409~424.

Schobert, H., 1962, "Sitzhaltung, Sitzschaden, Sitzmöbel," Springer-Verlag, Berlin.

Schultz, A., Andersson, G., Örtengren, R., Haderspeck, K. and Nachemson, A., 1982, "Loads on the Lumbar Spine : Validation of a Biomechanical Analysis by Measurements of Intradiscal Pressures and Myoelectric Signals," J. Bone Jt Surg., Vol. 64(A), pp. 713~720.

Schultz, A., Haderspeck, K., Warwick, D. and Portillo, D., 1983, "Use of Lumbar Trunk Muscles in Isometric Performance of Mathematically Complex Standing Tasks," J. Orthop. Res., Vol. 1, pp. 77~91.

Seireg, A. and Arvikar, R.J., 1973, "A Mathematical Model for Evaluation of Forces in Lower Extremities of the Musculo-Skeletal System," J. Biomechanics, Vol. 6(3), pp. 313~326.

Shoemaker, S.C. and Markolf, K.L., 1985, "Effects of Joint Load on the Stiffness and Laxity of Ligament-Deficient Knees : An in Vitro Study of the Anterior Cruciate and Medial Collateral Ligaments," J. Bone Jt Surg., Vol. 67(A), pp. 136~146.

Siegler, S., Moskowiz, G.D. and Freedman, W., 1984, "Passive and Active Components of the Internal Moment Developed about the Ankle Joint during Human Ambulation," J. Biomechanics, Vol. 17(9), pp. 647~652.

Son, K., 1988, "Biomechanical Analysis of Weight-Moving Tasks in the Seated Position," Ph.D. Dissertation, Univ. of Michigan, Ann Arbor, Michigan.

Son, K., Miller, J.A.A. and Schultz, A.B., 1988, "The Mechanical Role of the Trunk and Lower Extremities in a Seated Weight-Moving Task in the Sagittal Plane," ASME J. Biomech. Eng., Vol. 110(2), pp. 97~103.

Son, K. and Miller, J.A.A., 1988, "A Two-Dimensional Biomechanical Model for Predicting Trunk and Lower Extremity Muscle Activity in a Dynamic, Seated Task : A Quantitative Comparison of Optimization Schemes," in J. Stein (ed.), Modeling and Control Issues in Biomechanical Systems, DSC-Vol. 12, ASME, New York, pp. 103~120.

Son, K., 1990, "A Quantitative Analysis of Myoelectric Signals for Validating Muscle Forces Predicted by a Biomechanical Model," Research Report (College of Eng., Pusan National Univ.), Vol. 40, pp. 5~15.